Migration of noble gas atoms in interaction with vacancies in silicon

2015 Semicond. Sci. Technol. 30 085022

(http://iopscience.iop.org/0268-1242/30/8/085022)

IOP Publishing Semiconductor Science and Technology
Semicond. Sci. Technol. 30 (2015) 085022 (8pp) doi:10.1088/0268-1242/30/8/085022

Migration of noble gas atoms in interaction with vacancies in silicon

L Pizzagalli[1] and A Charaf-Eddin[2]

[1] Department of Physics and Mechanics of Materials, Institut P', CNRS—Université de Poitiers UPR 3346, SP2MI, BP 30179, F-86962 Futuroscope Chasseneuil Cedex, France
[2] CINaM, CNRS UMR 7325, Campus de Luminy, Case 913, 13288 Marseille Cedex 9, France

E-mail: Laurent.Pizzagalli@univ-poitiers.fr

Received 9 March 2015, revised 30 June 2015
Accepted for publication 1 July 2015
Published 28 July 2015

Abstract

First principles calculations in combination with the nudged elastic band method have been performed in order to determine the mobility properties of various noble gas species (He, Ne, Ar, Kr, and Xe) in silicon, a model semiconducting material. We focussed on single impurity, in interstitial configuration or forming a complex with a mono- or a di-vacancy, since the latter are known to be present and to play a key role in the formation of extended defects like bubbles or platelets. We determined several migration mechanisms and associated activation energies and have discussed these results in relation to available experiments. In particular, conflicting measured values of the migration energy of helium are explained by the present calculations. We also predict that helium diffuses solely as an interstitial, while an opposite behaviour is found for heavier species such as Ar, Kr, and Xe, with the prevailing role of complexes in that case. Finally, our calculations indicate that extended defects evolution by Ostwald ripening is possible for helium and maybe neon, but is rather unlikely for heavier noble gas species.

Keywords: noble gas, diffusion, silicon, density functional theory

(Some figures may appear in colour only in the online journal)

1. Introduction

Noble gas (NG) species, especially helium and argon, are essential components in various aspects of semiconductor processing. They are used during growth or in more specialized defect engineering processes. For instance, helium has been shown to be useful for gettering applications [1], where cavities formed after NG implantation [2–7] can be used to trap impurities coming from active layers of the future device. This phenomenon is also beneficial for relaxing strain in pseudomorphic SiGe/Si heterostructures, and an essential step in the smartcut process used in the production of silicon-on-insulator wafer substrates. Another use is the processing of surfaces by ion beam milling, and metallization, using inexpensive argon. Furthermore, imaging and nanomachining of semiconductors could be performed using the helium ion microscope [8].

To improve the efficiency of these processes and applications, it is highly desirable to achieve a better understanding of the interaction of NG atoms with semiconductors. One objective is to determine the structure, stability and mobility of single NG atoms in the material, starting at the atomic scale, which is what motivated the investigations reported here. We focussed on silicon, rightly considered as the archetypal semiconductor, and the one for which most information is available in the literature. There have been several studies, especially in the case of helium, reporting on the structural and stability properties [9–14]. However, the knowledge is much more scarce regarding the mobility properties. On the one hand, there have been conflicting measurements of migration energies [15–17]. On the other hand, previous theoretical works determined the migration of interstitial NG atoms, although we know now that for heavier NG species such as Kr and Xe, the interstitial configuration is not stable [13]. As a consequence, migration mechanisms leading to extended defect formation are still not identified.

In this work, we report on the mobility properties of a single NG atom in silicon, interacting or not with mono- and di-vacancy, investigated using density functional theory calculations. Several migration mechanisms and associated

energies for the different possible configurations are described, and discussed in relation to available experiments. In particular, our results allow us to identify the migration mechanisms in agreement with several diffusion experiments, as well as to remove a discrepancy in the case of helium. After a brief summary of the methods used, we describe possible migration mechanisms corresponding to the different configurations of a NG atom in the cubic diamond lattice. Then we detail the results obtained in the case of helium, neon, argon, krypton and xenon.

2. Methods

The theoretical framework considered in this work has been described in detail and validated in a recent paper [13], and only the essential information will be recalled here. The migration properties of NGs in silicon were determined from density functional theory numerical simulations, performed using the PWscf code [18] from the Quantum ESPRESSO project [19]. The Perdew–Burke–Ernzerhof generalized gradient approximation (GGA-PBE) [20] was used for exchange and correlation contributions. We used a plane wave cutoff of 15 Ry and a $\frac{1}{2}$-shifted 2^3 Monkhorst–Pack grid of k-points [21], equivalent to a set of four irreducible k-points. This leads to a silicon lattice parameter $a_0 = 5.468$ Å.

Systems were modelled in a $3a_0 \times 3a_0 \times 3a_0$ periodically repeated cubic supercell. With this setup, we computed formation energies of 3.33 eV and 5.05 eV for the mono- and di-vacancy in silicon, respectively. The dissociation of the di-vacancy then required 1.61 eV, a value in excellent agreement with previous calculations [22].

The energies needed to accommodate a NG atom in various locations are reported in table 1 (see [13] for full description of configurations). The determination of migration properties was achieved by employing the nudged elastic band (NEB) method [23, 24], with four or five fully optimized replicas. Guesses for initial paths were made by linear interpolation in the case of simple mechanisms, or built by hand in the case of exchange mechanisms. Two successive NEB calculations were done. In the first one, all replicas were equivalently optimized until convergence. The result was used as input for the second calculation where the replica with the highest energy was allowed to climb along the path in order to refine the determination of the saddle point and migration energy [25].

3. Migration mechanisms

The various possible stable configurations for each NG species are described in our previous work [13]. The migration mechanism that received the most attention in earlier studies is probably the direct straight path between two T sites. The position midway is the unstable or weakly stable H site (figure 1). The latter is assumed to be the saddle point along the minimum energy path (MEP), which allows for an easy

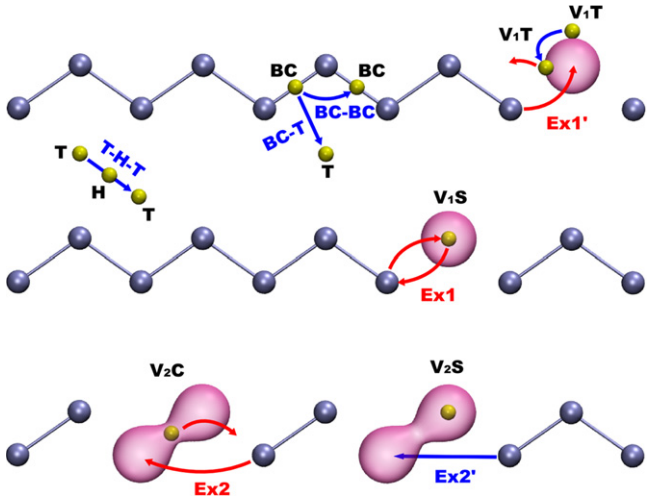

Figure 1. Some possible configurations for a NG atom (yellow sphere) as interstitial or interacting with mono- and di-vacancies (transparent pink volume), projected in a {110} silicon (blue spheres) layer. Migration paths are shown as blue or red arrows, depending whether they concern a single NG or silicon atom, or concerted displacement of both species. See table 1 and section 3 for further explanations on notations.

Table 1. Energies (in eV) required to introduce a single NG atom into the silicon lattice. For interstitial configurations, tetrahedral (T), hexagonal (H), split (SP), and bond centered (BC). For mono-vacancy, NG at the centre (V_1S) or in the first neighbor tetrahedral site (V_1T). For di-vacancy, NG at the centre (V_2C), or at one of the vacancy centres (V_2S). The '–' symbol indicates unstable or untested configurations.

	He	Ne	Ar	Kr	Xe
T	1.00	2.50	5.83	7.14	10.22
H	1.66	3.37	6.86	8.02	10.82
BC	–	–	5.81	5.82	7.14
SP	–	–	7.13	6.96	–
V_1S	1.82	1.98	2.63	2.29	3.34
V_1T	1.15	1.65	–	–	–
V_2S	–	–	1.63	1.24	2.30
V_2C	0.49	0.89	–	1.94	2.54

calculation of the energy barrier as the difference between T and H insertion energies [9, 11]. This assumption has been verified using NEB calculations [12]. The T-H-T mechanism has been calculated for all NG species. In all cases, it was found that the silicon lattice keeps its integrity while the impurity migrates. The largest lattice deformations are obtained for heavier NG species, whereas helium seems to move without any apparent distortions (figure 2).

In diamond, Goss and co-workers have investigated the migration path for an Ar, Kr and Xe interstitial in a split (SP) configuration, which is the most stable one for these species [26]. Midway between two SP sites, the NG atom has been found to be in a BC configuration. But in silicon, our calculations revealed that BC was more stable than SP for Ar, Kr, and Xe (table 1). Accordingly, we have investigated the migration path between two BC configurations (figure 1). The calculated BC–BC mechanism is shown in figure 3. In the

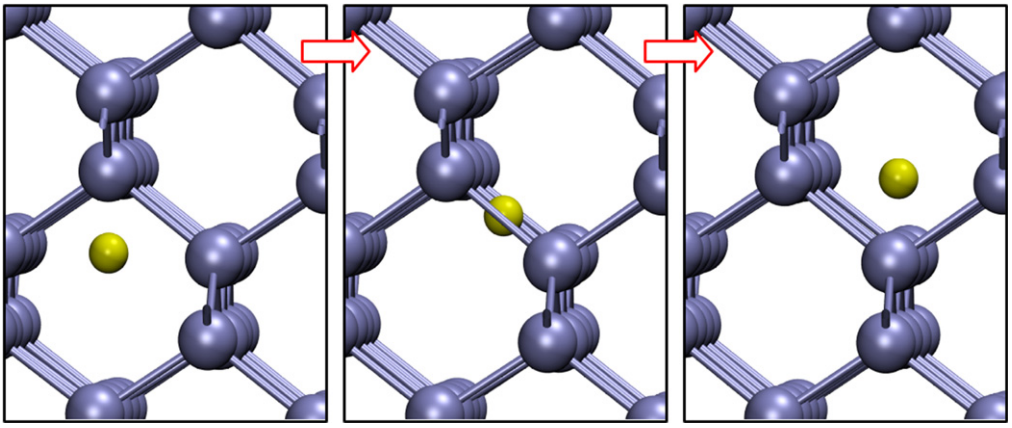

Figure 2. T-H-T migration mechanism, in the case of helium (yellow sphere). Si atoms are represented by blue spheres. The corresponding energy variation is shown in figure 6.

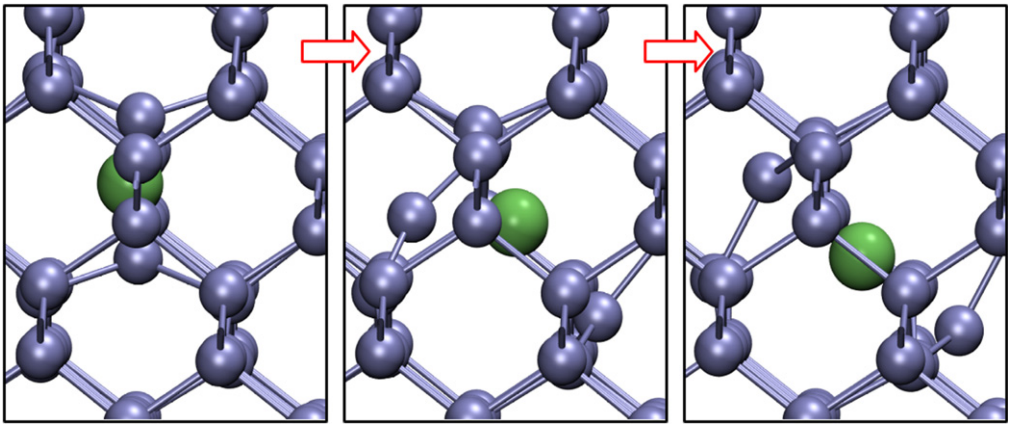

Figure 3. BC–BC migration mechanism, in the case of argon (green sphere). Si atoms are represented by blue spheres. The corresponding energy variation is shown in figure 6.

initial configuration, the NG atom is aligned with two largely displaced silicon atoms along the ⟨111⟩ direction. In the first steps, the NG atom and one of these two silicon atoms move in a concerted fashion, forming a SP configuration by lining up along a ⟨110⟩ direction mid-path. During the remaining steps, they continue to move until they are again aligned along another ⟨111⟩ direction, thus with a 109.47° rotation compared to the initial orientation. The remaining silicon atom comes back to the lattice site, while a new silicon atom is now displaced to form the BC configuration. This mechanism is probably similar to the one discussed in [26], with a reversed stability of SP and BC configurations.

The last interstitial migration mechanism that we have investigated is relevant to argon only. In fact, since almost equal insertion energies were found for BC and T configurations (table 1), we studied a possible BC–T path. The mechanism is characterized by the straight translation of the argon atom from the BC site to the T site. At the same time, the two initially strongly displaced silicon atoms tend to revert back to their original lattice sites. The geometry of the saddle point along the MEP bears no remarkable features.

We now turn to the cases where the NG atom is interacting with a mono- or a di-vacancy (NG-V_1 and NG-V_2). To our knowledge, no migration mechanisms have been previously proposed for NG-V_1 complexes in silicon. In the case of argon in substitution in diamond, calculations by Goss *et al* have revealed that migration would occur by an exchange mechanism for an activation energy of 5.9 eV [26]. A similar scenario has been obtained in the present work for NG species bound to the silicon mono-vacancy (figure 1). When the NG atom is in substitution, i.e. for Ar, Kr, and Xe, the Ex1 mechanism is characterized by the concerted displacements of the NG atom and a silicon atom initially first-neighbor of the vacancy, the displacements being essentially contained in a {110} plane (figure 4). The silicon atom reaches the initial vacancy location, leaving a vacant site finally occupied by the NG atom. The saddle point along the MEP resembles a BC-like configuration, with a Si-NG-Si alignment orientation slightly different from ⟨111⟩ due to the presence of the vacancy. The situation involving neon and a monovacancy is somewhat at variance since the NG atom is no longer at the vacancy centre. The proposed Ex1' mechanism is nevertheless quite similar to Ex1 (figure 1). The main differences are the shorter displacement of the neon atom, and the geometry at the saddle point which has no remarkable features.

Finally, we also investigated the case of a single NG atom interacting with a divacancy, for which no information

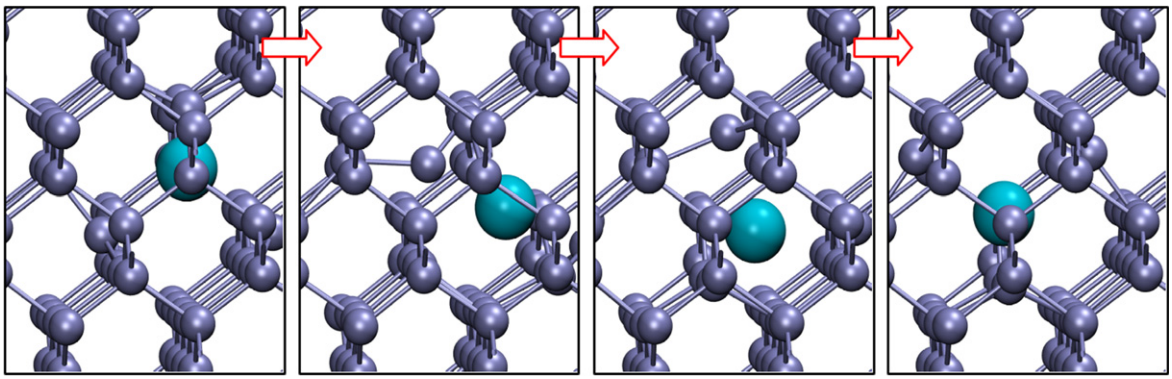

Figure 4. Ex1 migration mechanism, in the case of krypton (blue sphere). Si atoms are represented by blue spheres. The corresponding energy variation is shown in figure 6.

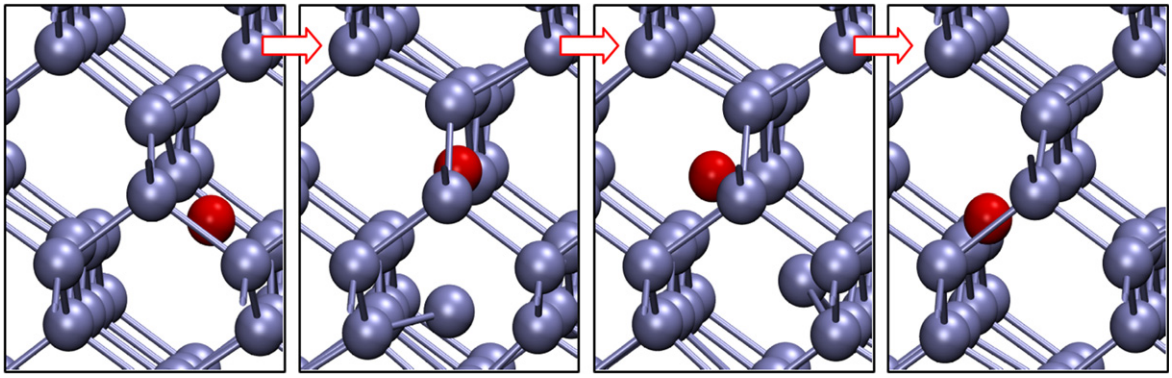

Figure 5. Ex2 migration mechanism, in the case of neon (red sphere). Si atoms are represented by blue spheres. The corresponding energy variation is shown in figure 6.

is available. Our calculations indicate that the mechanism with the lowest associated energy is essentially characterized by the displacement of a silicon atom initially first neighbor of the divacancy, which migrates until occupying the farthest vacancy centre (figure 1). This process leads to the displacement of the divacancy. When the NG atom is initially located at the divacancy centre (helium, neon), it migrates to reach the new divacancy centre, its motion being concerted with the moving silicon atom (Ex2). At the saddle point, the NG atom is located close to one vacancy centre, approximately aligned along the ⟨001⟩ direction with the moving silicon atom (figure 5). A slightly different scenario (Ex2', figure 1) is obtained when the NG atom is initially located at one vacancy centre (argon, krypton and xenon). In that case the NG atom stays close to this location during the relaxation. Also the previous saddle configuration now becomes metastable. At the new saddle points, the alignment between the NG atom and the moving silicon atom is now tilted by 13° relative to ⟨001⟩. During both Ex2 and Ex2' processes, all atomic displacements remain confined to a {110} plane, as for Ex1/Ex1'.

4. Helium

There have been several measurements of the activation energy for helium diffusion. Pioneering works by van Wieringen and Warmoltz lead to a value of about 1.35 eV for temperatures between 967 and 1207 °C [15]. A few years later, Luther and Moore reported a much lower value of 0.58 eV between 467 and 977 °C [16]. Finally, a sightly higher value of 0.80 eV was obtained in a similar temperature range of 300–900 °C [17]. Thus experiments suggest the existence of two regimes at high and low temperatures, with different activation energies.

Assuming that the activation energy for the diffusion of interstitial helium could be obtained as the energy difference of H and T configurations, Alatalo *et al* calculated with a first principles method a value of 0.84 eV [9], in agreement with measurements in the low temperature regime. However, later investigations using a similar framework lead to a higher value of 1.38 eV [11], in strikingly good agreement with the high temperature measurements of van Wieringen and Warmoltz [15]. More recent NEB first principles calculations involving the authors of this paper yielded a value of 0.71 eV [12], thus in agreement with the former study and with low temperature experiments.

The MEP obtained from our first principles NEB calculations are shown in figure 6. In the case of interstitial helium and a T-H-T diffusion mechanism, a value of 0.68 eV is determined for the activation energy (table 2). This value is slightly different to the value reported above, due to the use of a larger computational system. Besides, it is in excellent agreement with some of the previously

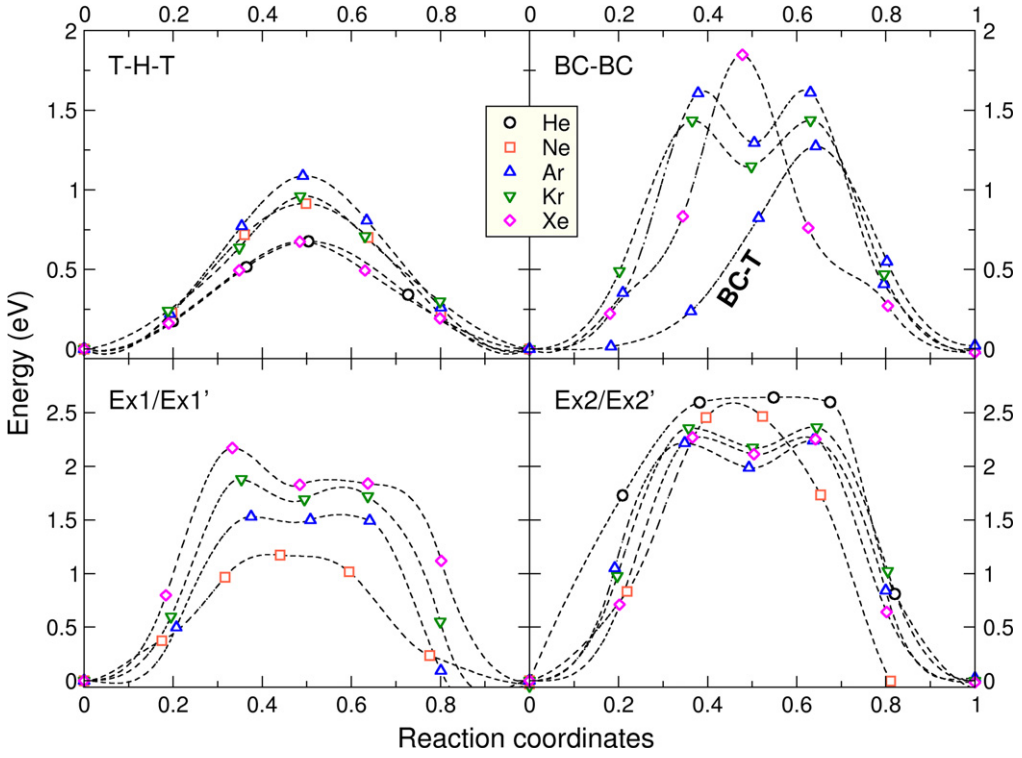

Figure 6. NEB calculated MEP for the mechanisms T-H-T, BC-BC, BC-T, Ex1/Ex1', and Ex2/Ex2' (see figure 1 and text for description). Replica energies are marked by black circles (helium), red squares (neon), blue triangles up (argon), green triangle down (krypton), and magenta diamond (xenon). Dashed lines have been generated using cubic or Akima splines in order to better display the MEP, yielding in a few cases negative energy values with no physical meaning. Asymmetrical MEP occurred due to the activation of a climbing image procedure during the relaxation.

Table 2. NEB computed activation energies (in eV) associated with different migration mechanisms of a single NG atom as interstitial, or in interaction with a mono- or a di-vacancy in silicon (see the text for meaning of labels). The '–' symbol indicates mechanisms not relevant for a given species.

	He	Ne	Ar	Kr	Xe
T-H-T	0.68	0.91	1.09	0.96	0.67
BC-BC	–	–	1.61	1.44	1.86
BC-T	–	–	1.26	–	–
Ex1/Ex1'	–	1.20	1.53	1.83	2.17
Ex2/Ex2'	2.64	2.53	2.26	2.36	2.24

published experimental data [16, 17], and confirms the interstitial character of diffusion in the low temperature regime.

The occurrence of He-V_1 complexes is very unlikely, since we found no attractive interaction between the helium atom and a monovacancy. However, the situation is different for the divacancy. A He-V_2 complex is predicted here to diffuse by the Ex2 mechanism with an activation energy of 2.64 eV (figure 6 and table 2). Since it is rather a high activation energy, it is interesting to investigate an alternative mechanism, where the helium dissociates from the divacancy and migrates as an interstitial. The associated activation energy is simply obtained in that case as the sum of the insertion energy of the helium atom in the T site plus the T-H-T migration energy minus the insertion energy of helium in V_2C configuration, i.e. $1.00 + 0.68 - 0.49 = 1.19$ eV. This is close to the measured activation energy of 1.35 eV for the diffusion of helium, which suggests that van Wierigen and Warmoltz actually measured the diffusion of helium atoms initially trapped in divacancies (or larger vacancy aggregates), but probably not the diffusion of interstitial helium [15]. This is further confirmed by the fact that they also measured a solution enthalpy of 0.46 eV, almost equal to our computed insertion energy of 0.49 eV for the helium atom in the divacancy (table 1).

Finally, activation energies of 1.7 eV [27], 1.8 eV [28], and 1.83 eV [3] for helium desorption from silicon bubbles have been measured using thermal desorption spectrometry. Recent calculations point to the fact that the activation energy could be approximately obtained as the sum of the insertion energy of the helium atom in the T site plus the T-H-T migration energy for interstitial desorption [29]. Using our values we obtained 1.68 eV, which is in good agreement with experimental data. Then, all the results presented here lead to the important conclusion that helium atoms always migrate as interstitials in silicon, even if trapped in vacancy aggregates V_n (with $n \geqslant 2$) and bubbles. It implies that possible bubble coarsening by the Ostwald ripening process would rely on separate exchanges of interstitial helium atoms and vacancies, and not of small He_nV_m complexes.

5. Neon

To the best of our knowledge, quantitative experimental data on the diffusion of neon in silicon are not available. Only calculations have been performed, yielding values of 2.03 eV [11] and 1.00 eV [12] for the diffusion of the interstitial neon atom. In this work we obtained a better converged energy of 0.91 eV by using a larger computational system (table 2). This value is only 0.23 eV larger than the migration energy for helium, thus hinting that the interstitial neon is also mobile at moderate temperatures. However, van Wierigen and Warmoltz reported the absence of diffusion in their experiments [15]. A possible explanation is that neon atoms were already trapped by vacancies in their experiments, as for helium.

We analyze the different possible mechanisms leading to the diffusion of a single neon atom bound to mono- and di-vacancy. Figure 6 shows the Ex1' and Ex2 NEB computed MEP, with associated energies of 1.20 eV and 2.53 eV (table 2). Note that in the case of Ex1', the initial and final configurations are not symmetric by translation, since there are several equivalent V_1T positions for the neon atom as explained previously. We have computed the migration energy between two of these equivalent positions, and found a value of only 0.18 eV. This points to an easy motion of the neon atom around the monovacancy centre, with no influence on diffusion. We also considered the possible dissociation of the Ne-V or Ne-V_2 complexes, as in the helium case. Using insertion energies reported in table 1 and the neon interstitial migration energy of 0.91 eV, we found that the activation energy for Ne-V dissociation followed by the migration of the interstitial neon atom is 1.76 eV. This value is significantly higher than 1.20 eV, our NEB calculated energy for the migration of the Ne-V complex by the exchange mechanism Ex1'. It is then likely that the latter mechanism is favoured. Considering now the dissociation of the Ne-V_2 complex followed by the migration of the neon interstitial, an activation energy of 2.52 eV is obtained, thus quasi equal to the migration energy of the Ne-V_2 complex by the Ex2 mechanism. In that case, we are not able to discriminate in favour of one of the two processes.

At last, our calculations showed that the activation energy for the desorption of interstitial neon atoms from large bubbles would be at least about 3.4 eV (assuming that the insertion energies in these bubbles are negligible). Another option is the emission of Ne-V_1 or Ne-V_2 complexes. With the same hypothesis of negligible neon insertion energy in large bubbles, and also of low binding energies for mono- and di-vacancies to bubbles, we determined activation energies of 3.42 eV and 2.85 eV for these mechanisms. These are in the same range as the energy for interstitial emission, i.e. large enough to explain why no neon desorption was observed conversely to the helium case [15]. This also hints that the evolution of Ne-filled bubbles by exchange of interstitial neon atoms or Ne-$V_{1|2}$ complexes is possible but rather unlikely. Bubble coarsening by migration and coalescence processes [30] is certainly favoured here.

6. Argon

Argon diffusion in silicon has been investigated by thermal desorption spectrometry [31, 32], reporting several activation energies of 1.47 eV, 2.35 eV, and 3.91 eV. Theoretically, only the migration of the interstitial argon atom by the T-H-T mechanism has been calculated, with values of 1.21 eV [12] and 3.51 eV [11]. Our calculations lead to a lower value of 1.09 eV for this mechanism (figure 6 and table 2), essentially because of the system size argument already discussed. It is also found that T and BC configurations were quasi-degenerate in energy. Then we have computed the MEP corresponding to the migration between two BC configurations, and between BC and T (figure 6). In the former case, a metastable intermediate SP configuration is obtained. We determined activation energies of 1.61 eV (BC–BC) and 1.26 eV (BC–T). These results reveal that the diffusion of interstitial argon atoms is likely to proceed by the T–H–T mechanism, and that an argon atom in BC configuration could switch to a T site within the same range of temperature as T–H–T interstitial diffusion.

Considering now the interaction with the monovacancy, we found that the substitutional argon atom will diffuse with an activation energy of 1.53 eV. The dissociation plus interstitial migration process requires a much higher energy of 4.29 eV, severely limiting its occurrence. The same conclusion applies for the dissociation of the Ar-V_2 complex in Ar +V_2 or in Ar-V_1+V_1, for which large activation energies of 5.29 eV and 4.14 eV are determined. The latter value is calculated as the sum of the insertion energy of argon atom in V_1S minus the insertion energy in V_2S plus the dissociation energy of the divacancy and the migration energy of the Ar-V_1 complex, i.e. $2.63 - 1.63 + 1.61 + 1.53 = 4.14$ eV. The last possible case is the migration of the Ar-V_2 complex. NEB calculations yielded an activation energy of 2.26 eV for the Ex2' mechanism (figure 6 and table 2). Since the argon atom prefers to sit at one vacancy centre, we also computed the energy barrier for the argon diffusion inside the divacancy, from one vacancy centre to the other, within the same approach. We obtained a low value of 0.31 eV, suggesting that the argon atom would easily move inside the divacancy in usual conditions.

After comparing our calculated values with the available measurements, it is tempting to conclude that the 1.47 eV value from Hanada *et al* [31] corresponds to the diffusion of substitutional argon by the Ex1 mechanism (calculated activation energy of 1.53 eV). This view is reinforced by the fact that argon implantation, even at low fluence, is necessarily associated with a substantial creation of vacancies in the silicon lattice. Also, the formation of the Ar-V_1 complex from thermally activated vacancies requires an energy comparable to the insertion energy of the interstitial argon atom [13]. The second measured energy, 2.35 eV, could be identified to the calculated activation energy of 2.26 eV for the diffusion of the Ar-V_2 complex by the Ex2' mechanism. Finally, for the third measured value of 3.91 eV, three possible mechanisms could be considered. In the first one, the energy would correspond to the dissociation plus interstitial migration of the

Ar-V_1 complex, determined here to be 4.29 eV. A second option would be the dissociation of the Ar-V_2 complex in Ar-V_1+V_1 followed by the migration of the Ar-V_1 complex. Finally, an alternative scenario is the formation and migration of an Ar-V_2 complex from a large Ar-filled bubble. Assuming that both the argon insertion energy and the vacancy binding energy are negligible in such a bubble, the activation energy of the process would be simply the sum of the insertion energy for Ar in V_2 and of the Ex2' mechanism, i.e. 3.89 eV, very close to the measured data. Obviously, one has to be cautious here, since it is always possible to get good agreement when combining several numbers. Furthermore, Hirashita reported that his measured energies were concomitant to crystallization of damaged layers and microstructural evolution [32].

To conclude about argon, our investigations suggest the prevailing role of Ar-V_1 and Ar-V_2 complexes. The general picture is that argon interstitials have a limited lifetime and are quickly trapped by mono- or di-vacancies, either due to the implantation damage or being thermally activated. The desorption of argon from bubbles would rely on the emission of these complexes. As a result, Ar-filled bubbles are predicted to shrink together with argon desorption.

7. Krypton

It seems that the only published investigation of krypton desorption following implantation in silicon was performed more than 40 years ago by Matzke [33]. He measured two activation energies of 1.8 eV and 3.5 eV, depending on the implantation conditions. Regarding calculations, only the T–H–T migration mechanism has been investigated [11, 12] as for the case of argon. However, this mechanism is not relevant since a BC configuration is favoured for the krypton interstitial [13]. The interstitial migration should operate through the BC–BC mechanism, which also includes a metastable SP configuration midway (figure 6). The associated activation energy is 1.44 eV, thus lower than experimental values.

Similarly to argon, the lifetime of the krypton atom in interstitial configuration is necessarily limited, ultimately leading to the formation of Kr-$V_{1|2}$ complexes with vacancies thermally activated or resulting from the implantation process. For substitutional krypton, i.e. Kr-V_1, an activation energy of 1.83 eV is determined for the migration by the Ex1 mechanism (figure 6 and table 2). This value is in excellent agreement with the lowest measured data, making the migration of the Kr-V_1 complex a good candidate to explain the first experimental regime. The dissociation plus interstitial migration process requires a large energy of 4.97 eV instead. The migration of Kr-V_2 by the Ex2' mechanism has been calculated, yielding an activation energy of 2.36 eV (table 2). In addition, an activation energy of 0.70 eV has been computed for the migration of the krypton atom between vacancy centres in the divacancy. The dissociation of this complex, leaving the Kr atom migrating either as an interstitial or in substitution, requires energies of 6.02 eV and 4.49 eV, respectively.

None of these values seem to match the second measured data by Matzke [33]. However, if we follow the same reasoning as for argon, an estimated energy of 3.60 eV is obtained for the emission of a Kr-V_2 complex from large Kr-filled bubbles. A larger energy of 4.12 eV would be required for the emission of a Kr-V_1 complex. Our results then suggest a picture almost similar to the case of argon, diffusing species being NG-V_1 and NG-V_2 complexes. The sole difference is the absence of experimentally reported values corresponding to the Kr-V_2 diffusion by the Ex2' mechanism.

8. Xenon

The issue with xenon is that, to our knowledge, no measurements of diffusion or desorption have been made. From the theory side, only the activation energies for interstitial diffusion by the T–H–T mechanism have been calculated [11, 12]. As for krypton, this information is not relevant since we have previously shown that the interstitial xenon atom would be in a BC configuration. Instead, our calculations revealed that interstitial xenon migration would occur through a BC–BC mechanism, with no stable SP configuration along the path (figure 6), and an activation energy of 1.86 eV. However, the probability of a xenon atom in interstitial configurations is even lower than for argon and krypton [13].

Interestingly, we found almost the same activation energies of 2.17 eV and 2.24 eV for the migration of Xe-V_1 and Xe-V_2 complexes by the Ex1 and Ex2' mechanisms, respectively (figure 6 and table 2). Thus, despite the size of the xenon atom, its motion into the silicon lattice requires moderate energies as long as it is bound to a mono- or a divacancy. In the case of the Ex2' mechanism, we additionally found that the xenon atom could migrate inside the divacancy with an energy barrier of 0.35 eV. Considering now diffusion by dissociation plus interstitial migration processes, we found that large energies are needed in any case. Hence, we calculated a value of 5.66 eV for the dissociation of Xe-V_1 followed by interstitial xenon migration. For Xe-V_2, a similar process requires 6.7 eV, and 4.82 eV if the migrating species is a substitutional xenon after dissociation. Xe-$V_{1|2}$ complexes then appear to be quite stable against dissociation. Finally, doing the same analysis as for previous NG species, we determined energies of 5.51 eV and 4.54 eV for the emission of Xe-V_1 and Xe-V_2 complexes from large xenon-filled bubbles.

9. Conclusions

We have investigated the mobility of single NG atoms in pristine silicon, and in interaction with a mono- and a divacancy, using density functional theory calculations and the NEB method. This allowed us to determine migration mechanisms and associated activation energies for various

starting configurations. Our results have helped to solve an apparent discrepancy between different activation energy measurements for helium diffusion in silicon. In fact, we show that one value is related to the migration of helium interstitial initially trapped by vacancies (V_2 or larger aggregates), while the other set is simply related to the migration of untrapped interstitials. Our calculations also revealed the prevailing role of the interstitial helium compared to complexes, the former being probably the only possible diffuser. The heaviest NG species, argon, krypton and xenon, show the opposite behaviour. Once formed, NG-$V_{1|2}$ complexes are very stable against dissociation, and migrate as single entities. Neon is an intermediate case. Similar activation energies have been calculated for diffusion by dissociation processes or by the migration of complexes.

Regarding the evolution of large NG-filled bubbles, our results would suggest that bubble coarsening by Ostwald ripening is only possible for helium and maybe neon, with exchanged species being interstitial atoms and vacancies. For heavier gas, the large computed energies make the emission from bubbles of interstitials or small NG-$V_{1|2}$ complexes quite unlikely, in comparison with migration and coalescence processes which should weakly depend on the nature of the embedded noble gas.

In this work, all the mobility energy values were computed without considering temperature effects such as additional vibrational energy contributions. But it is important to recall that the latter are expected to be quite low, since mobility energies are calculated by comparing very similar configurations thus leading to an efficient cancellation of thermal dependent quantities. Nevertheless, it would be interesting to perform further calculations to confirm this point.

Acknowledgments

Figures 1–5 were made with VMD software support. VMD is developed with NIH support by the Theoretical and Computational Biophysics group at the Beckman Institute, University of Illinois at Urbana-Champaign.

References

[1] Raineri V, Battaglia A and Rimini E 1995 *Nucl. Instrum. Methods Phys. Res.* B **96** 249
[2] Cerofolini G F, Corni F, Frabboni S, Nobili C, Ottaviani G and Tonini R 2000 *Mater. Sci. Eng. Reports* **27** 1
[3] Oliviero E, David M L, Beaufort M F, Barbot J F and van Veen A 2002 *Appl. Phys. Lett.* **81** 4201
[4] Beaufort M F, Pizzagalli L, Gandy A S, Oliviero E, Eyidi D and Donnelly S E 2008 *J. Appl. Phys.* **104** 094905
[5] David M L, Barbot J F, Rousselet S, Pailloux F, Beaufort M F, Pizzagalli L, Drouet M, Simoen E R and Claeys C 2008 *ECS Trans.* **16** 163
[6] David M L, Pailloux F, Mauchamp V and Pizzagalli L 2011 *Appl. Phys. Lett.* **98** 171903
[7] Pizzagalli L, David M L and Bertolus M 2013 *Modelling Simul. Mater. Sci. Eng.* **21** 065002
[8] Livengood R H, Greenzweig Y, Liang T and Grumski M 2007 *J. Vacuum Sci. Technol.* B **25** 2547–52
[9] Alatalo M, Puska M J and Nieminen R M 1992 *Phys. Rev.* B **46** 12806
[10] Allen W R 1994 *J. Nucl. Mater.* **210** 318
[11] Estreicher S K, Weber J, Derecskei-Kovacs A and Marynick D S 1997 *Phys. Rev.* B **55** 5037
[12] Charaf Eddin A, Lucas G, Beaufort M F and Pizzagalli L 2009 *Comput. Mat. Sci.* **44** 1030
[13] Pizzagalli L, Charaf-Eddin A and Brochard S 2014 *Comput. Mat. Sci.* **95** 149–58
[14] Pizzagalli L, David M L and Charaf-Eddin A 2015 *Nucl. Instrum. Methods Phys. Res.* B **352** 152–5
[15] van Wieringen A and Warmoltz N 1956 *Physica* **22** 849
[16] Luther L C and Moore W J 1964 *J. Chem. Phys.* **41** 1018–26
[17] Jung P 1994 *Nucl. Instrum. Methods Phys. Res.* B **91** 362
[18] Giannozzi P *et al* 2009 *J. Phys. Condens. Matter* **21** 395502
[19] Http://quantum-espresso.org/
[20] Perdew J P, Burke K and Ernzerhof M 1996 *Phys. Rev. Lett.* **77** 3865
[21] Monkhorst H J and Pack J D 1976 *Phys. Rev.* B **13** 5188
[22] Caliste D and Pochet P 2006 *Phys. Rev. Lett.* **97** 135901
[23] Jónsson H, Mills G and Jacobsen K W 1998 Nudged elastic band method for finding minimum energy paths of transitions *Classical and Quantum Dynamics in Condensed Phase Simulations* ed B J Berne, G Ciccotti and D F Coker ch 16 (Singapore: World Scientific) p 385
[24] Henkelman G and Jónsson H 2000 *J. Chem. Phys.* **113** 9978
[25] Henkelman G, Uberuaga B P and Jónsson H 2000 *J. Chem. Phys.* **113** 9901
[26] Goss J, Eyre R, Briddon P and Mainwood A 2009 *Phys. Rev.* B **80** 085204
[27] Griffioen C, Evans J, Jong P D and van Veen A 1987 *Nucl. Instrum. Methods Phys. Res.* B **27** 417
[28] Godey S, Ntsoenzok E, Sauvage T, van Veen A, Labohm F, Beaufort M F and Barbot J F 2000 *Mater. Sci. Eng.* B **73** 54
[29] Charaf Eddin A and Pizzagalli L 2012 *J. Phys. Condens. Matter* **24** 175006
[30] Evans J 2002 *Nucl. Instrum. Methods Phys. Res.* B **196** 125–34
[31] Hanada R, Saito S, Nagata S and Yamaguchi S 1995 *Mater. Sci. Forum* **196–201** 1375
[32] Hirashita N 1999 *Japan. J. Appl. Phys.* **38** 613
[33] Matzke H 1970 *Radiat. Eff.* **3** 93–105